Int J Adv Manuf Technol (2018) 95:597–608
https://doi.org/10.1007/s00170-017-1218-9

ORIGINAL ARTICLE

A simple approach for analysing the surface texture transfer in cold rolling of metal strips

Chuhan Wu[1] · **Liangchi Zhang**[1] · **Peilei Qu**[2] · **Shanqing Li**[2] · **Zhenglian Jiang**[2]

Received: 27 June 2017 / Accepted: 16 October 2017 / Published online: 29 October 2017

Abstract This paper presents a simple approach for analysing the surface texture transfer in cold rolling of metal strips. The approach made use of the advantages of the slab method and accommodated the surface roughness effect of a rigid work roll. A numerically generated rough surface, whose heights generally follow a Gaussian distribution and distribute transversely, was used in the calculation. The transient distribution of contact stresses and instant texture transfer were then predicted. The interface contact pressure and friction stresses predicted by the established method were verified by the finite element method under the same rolling conditions. It was found that the new approach is efficient and cost-effective. The application of the approach revealed that due to the surface texture of the work roll, the interface stress in the rolling bite can be discontinuous, and that a higher roughness transfer ratio can be expected when reduction ratio increases.

Keywords Texture transfer · Roughness effect · Slab method · Cold rolling

Nomenclature

c_a	Coulomb friction coefficient
E_s	Plane-strain Young's Modulus
δ	Local roughness amplitude of a rigid roll surface
Δt	Time increment
l	Current slab length in rolling
μ_a	Interface friction coefficient
q	Interface contact pressure
R	Roll radius
R_q	Surface roughness of the rolled strip
$R_{q,\,\mathrm{roll}}$	Surface roughness of the rigid roll
σ_x	Longitudinal stress of the slab
σ_y	Stress at the slab surface
τ	Interface friction stress
u_1	Strip velocity at the entry point
V_1	Moving speed at the left hand side of the slab
V_2	Moving speed at the right hand side of the slab
V_{ave}	Average moving speed of the slab
V_{exp}	Expansion velocity of each slab
V_{crit}	Critical relative sliding speed
v_s	Poisson's ratio
y	Strip half thickness
Y	Plane-strain yielding strength of the strip material
Y_a	Uniaxial yielding strength
y_0	Reference half strip thickness
y_{un}	Strip thickness at completely unloading state of the slab

1 Introduction

The surface roughness of a work roll plays a critical role in determining the surface finish of a rolled strip. In practice, the roll surface hardness is much higher than that of a metal strip; hence the surface texture of the former is prone to be transferred to the surface of the latter. To date, most investigations are based on steady rolling analyses, assuming that the

✉ Liangchi Zhang
Liangchi.Zhang@unsw.edu.au

[1] School of Mechanical and Manufacturing Engineering, The University of New South Wales, Sydney, NSW 2052, Australia

[2] Baoshan Iron & Steel Co., Ltd., Shanghai 200941, China

interface stress and strip thickness in the rolling bite does not vary with time. In reality, however, the rolling stress is non-steady and time-dependent, because texture transfer from a roll surface occurs instantly.

Extensive efforts have been made to characterise the rolling mechanism and explore the effects of surface roughness on rolling performance. To predict the distribution of interface contact pressure and friction stress in rolling bite, both slab method and finite element analysis (FEA) have been widely used. The slab method was developed based on Von Karman theory [1]. Due to its simplicity, it has been widely used to predict the roll-strip interface stress under simplified conditions [2–5], e.g., plane-strain and homogenous deformation. Compared with the slab method, the finite element analysis (FEA) can deal with complex constitutive models of materials in conjunction with more realistic boundary conditions [6–12].

Some efforts have also been made by using the slab method and FEA to examine the effect of surface roughness. Wilson and Sheu [13] studied the real contact area in a rolling bite based on the assumption of wedge-shape surface asperities. Sutcliffe [14] also developed a similar model to investigate the roughness effect on the interface stresses in rolling. By using the slab method and flattening model of the wedge-shape asperities, Wilson and Chang [15], Lin et al. [16] and Sutcliffe and Johnson [17] characterised the roughness effects on the mixed lubrication of cold rolling. However, the random contact of surface asperities was not considered in these works. Therefore, with the aid of the FEA and statistical characterisation of random asperity contact, Wu et al. [11, 12] developed an efficient method to analyse the interface stresses of randomly rough surfaces in lubricated contact sliding, which has enabled a unified avenue to deal with full film, mixed and boundary lubrication regimes and an effective multi-scale integration of the microscopic surface asperity deformation and the macroscopic bulk deformation of a workpiece.

While the surface roughness effects have been investigated to a certain extent, the influence of the texture transfer from a roll surface to a strip surface is missing. Moreover, it should be noted that the previous works aforementioned were based on steady rolling processes. Since the hardness of a roll surface is usually higher than that of a strip, the roll texture can be easily transferred to a strip surface. Experimental results have demonstrated that the roughness transfer from a roll surface to a strip surface can be considerably affected by operation conditions [18–20]. However, theoretical modelling of texture transfer is difficult. The finite element method has been used to predict the texture transfer in rolling. For instance, Kijima et al. [21–23] investigated the mechanism of roll-to-strip texture transfer at the skin pass. However, such a finite element analysis usually requires very fine mesh to capture the micro-scale surface morphology and is often restricted by the affordability of large-scale computations. Thus, a feasible and effective approach to investigate the roll-to-strip texture transfer and its effect on the rolling performance is required.

This paper aims to develop a simple approach to realise an efficient texture transfer analysis for cold rolling processes. A numerically generated rough surface with a Gaussian distribution of surface height will be used to explore the texture transfer process in rolling. By using the slab method in conjunction with hybrid boundary conditions, a deterministic method will be developed to explore the non-steady rolling associated with instant texture transfer and to enable an accurate determination of the transient interface stress variation with reduction ratio. In addition, a finite element analysis (FEA) will be used to verify the interface stresses and strip profile predicted by the simplified method proposed in this study.

2 Modelling

2.1 Governing equations

The stress equilibrium for each slab is shown in Fig. 1. By assuming a homogenous plane-strain deformation across the strip thickness, the governing equations of each slab can be written as [24]

$$d(y\sigma_x) = -qdy - \tau dx \tag{1}$$

$$\sigma_y dx = qdx - \tau dy \tag{2}$$

where σ_x is the longitudinal stress averaged over the strip thickness, q and τ are the interface normal contact pressure and friction stress, respectively, y is the strip half thickness and σ_y is the normal stress in the slab thickness direction. It should be noted that friction stress τ in Eqs. (1) and (2) can inverse its direction when the strip pass through the rolling bite. The coordinate system used in the analysis is also defined in Fig. 1. Under a dry surface contact, the interface contact pressure and friction stress can be related by

$$\tau = \mu_a q \tag{3}$$

where μ_a is the interface friction coefficient. As the strip is drawn into the rolling bite, a relative slip can occur between the roll and strip surfaces. 'Stick' happens when the relative sliding speed is zero. Hence, the stick-slip friction coefficient μ_a at the roll-strip interface can be described by a bi-linear stick-slip rule

$$\mu_a = sign\left(\frac{V_{roll} - V_{ave}}{V_{crit}}\right) c_a \text{ for } \frac{|V_{roll} - V_{ave}|}{V_{crit}} > 1 \tag{4}$$

$$\mu_a = c_a \frac{V_{roll} - V_{ave}}{V_{crit}} \text{ for } \frac{|V_{roll} - V_{ave}|}{V_{crit}} \le 1 \tag{5}$$

where c_a is the Coulomb friction coefficient for the complete sliding, V_{ave} is the average moving speed of the slab, V_{roll} is the

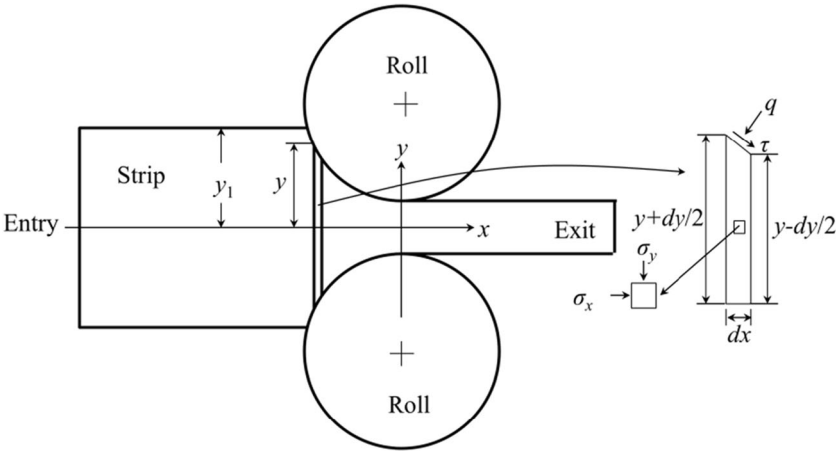

Fig. 1 Slab method for cold rolling

surface speed of work roll, V_{crit} is the critical relative sliding speed below which the stick occurs.

2.2 Loading/unloading processes

When a strip is drawn into the rolling bite, it undergoes both elastic and plastic deformations. In the elastic deformation regime, as illustrated in Fig. 2, the vertical elastic strain ε of the slab can be related to σ_y and σ_x by [25]

$$E_s\varepsilon(x) = \sigma_y - \frac{v_s}{1-v_s}\sigma_x \tag{6}$$

where v_s is Poisson's ratio, E_s is Young's Modulus under the condition of plane-strain, which is defined as $E/\left(1-v_s^2\right)$. Here, E is Young's Modulus of the strip material. It should be noted that the elastic strain is associated with the half strip thickness, y.

As the strip undergoes plastic deformation, as shown in Fig. 2, it is assumed that the yielding strength satisfies Tresca Yielding criterion [24]

$$\sigma_y - \sigma_x = 2Y \tag{7}$$

where Y is the yielding strength under plane strain condition.

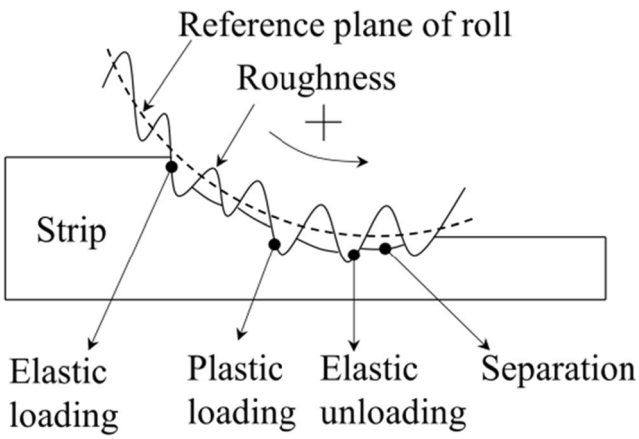

Fig. 2 Loading/unloading process

In cold rolling, unloading in a slab can occur because of the roll surface texture (see Fig. 2). The unloading process is elastic; thus

$$E_s\varepsilon_{un}(x) = \sigma_y - \frac{v_s}{1-v_s}\sigma_x \tag{8}$$

The strip thickness in the rolling bite is determined by both the geometry condition and the compression state. Hence, the elastic strain at unloading is determined by

$$\varepsilon_{un}(x) = \frac{y-y_{un}}{y_{un}} \tag{9}$$

where y_{un} is the strip thickness after the complete unloading of the slab without stress σ_y and σ_x. When the strip surface and roll surface are completely separated due to the microscale variation of the roll surface texture, stress σ_y on the non-contact zone becomes zero, as demonstrated in Fig. 2. Therefore, Eq. (8) reduces to

$$E_s\varepsilon_{un}(x) = -\frac{v_s}{1-v_s}\sigma_x \tag{10}$$

2.3 Boundary conditions

To solve the interface contact stress and friction stress governed by Eqs. (1) and (2), boundary conditions at the entry and exit are required. Generally, two types of boundary conditions can be applied to solve the equations:

(i) Constant inlet and outlet velocities of a strip with varied longitudinal stress at the entry and exit.
(ii) Constant longitudinal stresses at the entry and exit points with varied inlet and outlet velocities of a strip.

When the first type of boundary conditions is used, the inlet and outlet strip velocities are initially assumed. As the texture of a working roll passes through the rolling bite, σ_x at the entry

and exit points should be adjusted to satisfy the stress equilibrium equation. For the boundary conditions defined by the type (ii) above, σ_x at the entry and exit points are given at the beginning of numerical calculations. Then, the inlet and outlet velocities of a strip should be adjusted as the texture of a working roll is transferred to the strip. In this study, hybrid boundary conditions involving both the above two types of boundaries will be used in the numerical calculations. At the entry point, i.e., a constant moving speed is applied to the slab while $\sigma_{x,\ \text{outlet}}$ is applied to the slab at its exit. Overall, the hybrid boundary conditions can be described as follows:

$$V_{inlet} = u_1 \quad \text{at the entry point} \tag{11}$$

$$\sigma_{x,outlet} = \sigma_2 \quad \text{at the exit point} \tag{12}$$

where V_{inlet} is the entry speed at the entry, $\sigma_{x,\ \text{outlet}}$ is the longitudinal stress at the exit. Because of the hybrid boundary conditions involved in the numerical calculation, the longitudinal stress $\sigma_{x,\ entry}$ at the entry will be continually adjusted until the exit longitudinal stress $\sigma_{x,\ outlet}$ satisfies the predefined conditions. Then, the interface stress distribution and instant texture transfer are obtained.

2.4 Moving of rough surface texture

To simplify the analysis, only transverse surface roughness in the direction perpendicular to the rolling direction was considered. When the surface roughness of a rigid roll is considered, the time-dependent profile of a strip thickness in the rolling bite can be given by

$$y = y_0 + \frac{x^2}{2R} + \delta(x,t) \tag{13}$$

where y_0 is the reference half strip thickness at $x = 0$, R is the roll radius and δ is the roughness amplitude of a rigid roll surface. When the surface is smooth, the rolling process is at a steady state because the interface contact stresses do not vary with time. As the surface roughness is drawn into the rolling bite, the slab undergoes multiple loading-unloading cycles, which is governed by Eqs. (6) to (10).

2.5 Strip surface velocity

Based on the above discussion, it can be noted that the interface friction coefficient is dependent on the surface velocities of the roll and strip. When the strip is under rolling, the strip velocity can be decomposed into the squeezing velocity between slabs and the expansion velocity that was the result of the compression of each slab. By taking the slab shown in Fig. 3a as an example, the strip average velocity for a steady state rolling can be given by as follows;

$$V_{ave} = \frac{V_1}{\left(1-0.5y_i^{'}\frac{l}{y_i}\right)} \tag{14}$$

$$V_{\exp} = V_{ave}y_i^{'}\frac{l}{y_i} \tag{15}$$

$$V_2 = V_{ave} + V_{\exp}/2 \tag{16}$$

where V_{ave} is the average moving speed of the central position of the slab, V_1 and V_2 are the moving speeds on the left and right side of the slab, respectively, l is the current slab length in rolling, $V_{\exp}$ is the expansion velocity of each slab due to the compression of slab. In reality, V_1 and V_2 can be considered as the squeezing velocities between slabs.

When a steady state is obtained, the average moving speed of each slab within a time increment Δt, as illustrated in Fig. 3b, can be calculated by as follows:

$$V_{ave} = \frac{\Delta s}{\Delta t} = \frac{x(t) - x(t-\Delta t)}{\Delta t} \tag{17}$$

where $x(t-\Delta t)$ and $x(t)$ are the x coordinate of the slab at the beginning and end of time increment Δt, respectively. The x coordinate of the slab should be determined according to the loading-unloading cycle, plastic flow continuity and roll surface texture.

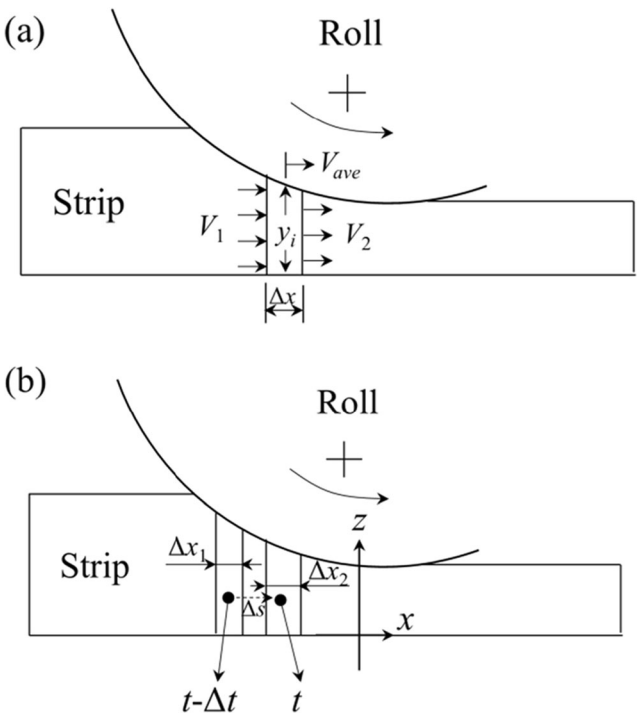

Fig. 3 Strip velocity calculation. **a** Steady state. **b** Transient state

3 Implementation

As discussed above, Eqs. (1) and (2) need to be solved by considering the hybrid boundary conditions defined by Eqs. (11) and (12) to obtain the longitudinal stress σ_x, interface normal contact pressure q and friction stress τ. Eqs. (1) and (2) are bounded by both the inlet and outlet boundaries, which brings about the difficulties in numerical calculation. Alexander [3] used the 4th Runge-Kutta method to integrate Eq. (1) from inlet to outlet. To consider both the inlet and outlet boundaries, the double shooting method [12, 15, 16] has been widely used by adjusting the neutral point. When the microscale roughness of roll surface is considered, the determination of neutral point becomes rather difficult. In this study, therefore, the governing equation will be solved from the entry to the exit in order to obtain the converged solution.

The overall numerical procedure for simulating the transient rolling process is given by the flow chart outlined in Fig. 4. The interface stresses and strip profile will be solved node by node from the entry to the exit of the rolling bite. The initial state of the calculation is with a smooth roll surface, as illustrated in Fig. 4b. Then, the calculation turns to the transient state by drawing the roughness roll surface into the rolling bite, as shown in Fig. 4a. At each time increment, the entry stress $\sigma_{x,\mathrm{entry}}$ is adjusted according to the boundary conditions. This can be easily achieved by using the obtained tension stress $\sigma_{x,\mathrm{exit}}$ at the exit and predefined tension stress $\sigma_{x,2}$, i.e.,

$$\sigma_{x,entry} = \sigma_{x,entry} + \omega\left(\sigma_{x,2} - \sigma_{x,exit}\right) \tag{18}$$

where ω is the relaxation factor for adjusting the entry tension stress. This process continues until the deviation ξ between $\sigma_{x,2}$ and $\sigma_{x,\mathrm{exit}}$ converges, i.e.,

$$\xi = \left|\sigma_{x,2} - \sigma_{x,exit}\right| \le \varepsilon \tag{19}$$

Then, the movement of the slab in the inlet zone can be determined by the entry velocity, i.e.,

$$\Delta x = u_1 \Delta t \tag{20}$$

Hence, the time increment in this step can be calculated as

$$\Delta t = \frac{\Delta x}{u_1} \tag{21}$$

The movement of the roll surface roughness within a small time increment Δt can be calculated by using Eq. (13). The above process repeats until the surface roughness completely passes through the rolling bite. During the calculation, the instant texture transfer from the roll to strip can be obtained in each time increment. Moreover, the overall distribution of the longitudinal stress σ_x, interface contact stress q and shear

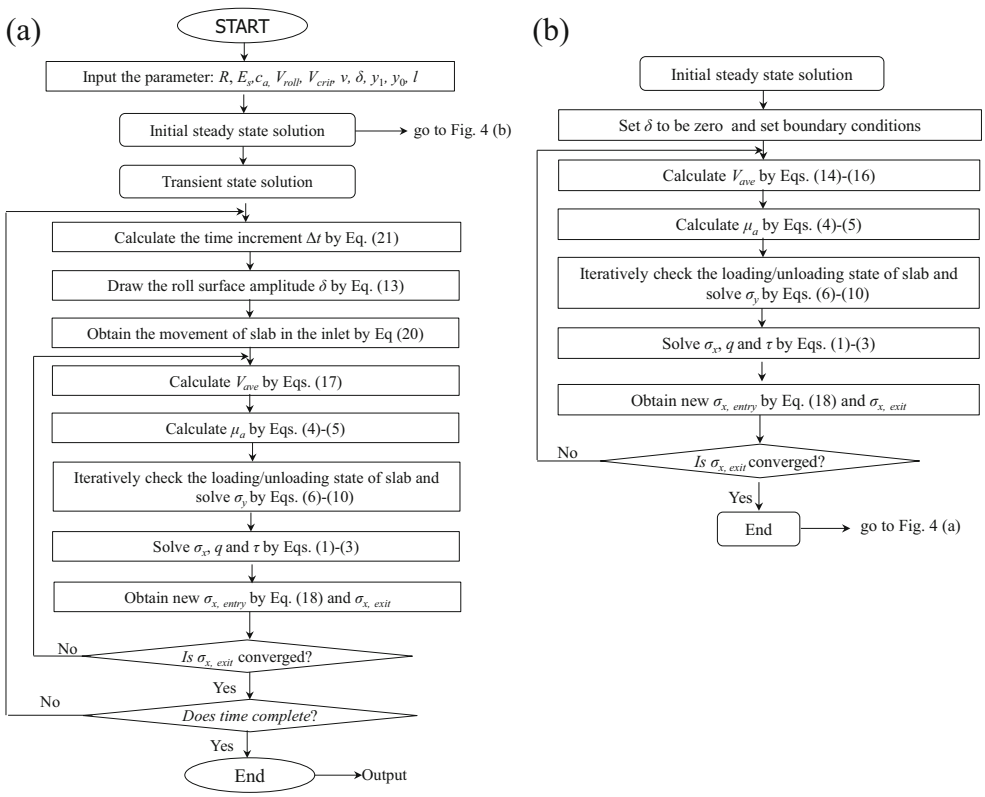

Fig. 4 Flow chart. **a** Numerical procedure for transient solution. **b** Numerical procedure for steady state solution

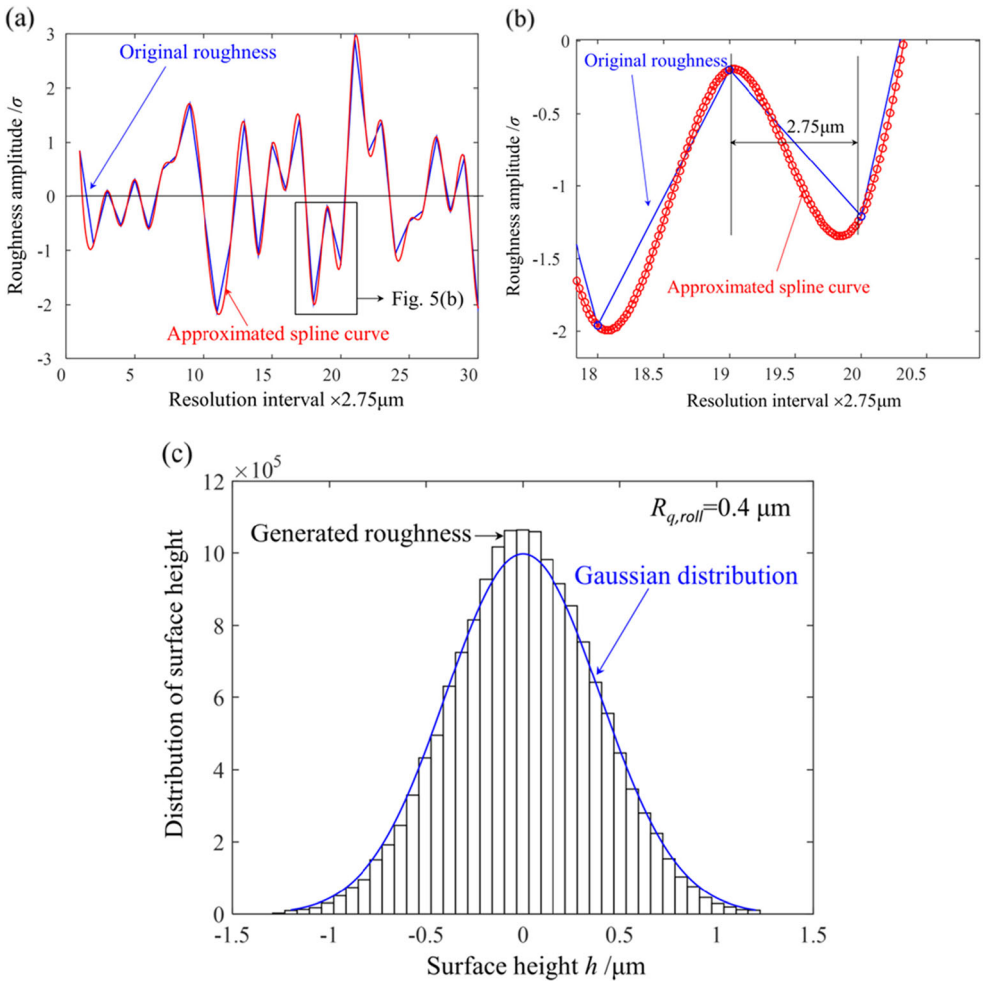

Fig. 5 Roll roughness. **a** Approximated surface roughness. **b** Resolution interval. **c** Height distribution of numerically generated rough surface

stress τ can be determined as well. It should be noted that the slab thickness in the rolling direction requires much finer discretisation compared with the roughness of a working roll in order to capture the roll-to-strip texture transfer. In this study, the resolution for working roll roughness is 2.75 μm and the initial width of each strip slab in the rolling direction is 0.1375 μm. During the calculation, the roll roughness is approximated by spline curves, as illustrated in Fig. 5a. The resolution of the approximated spline curves is also demonstrated in Fig. 5b.

To understand the topography of the numerically generated rough surface, its surface height distribution is compared with its statistical characteristics. The statistical characteristics were obtained by further processing the digital form of the generated rough surface. For most engineering surfaces, their surface heights usually follow a Gaussian distribution, i.e.,

$$f(h) = \frac{1}{R_{q,roll}\sqrt{2\pi}} \exp\left(-\frac{1}{2}\left(h/R_{q,roll}\right)^2\right) \tag{22}$$

where h is the surface height, $R_{q,\mathrm{roll}}$ is the calculated roughness of the generated rough surface.

Figure 5c clearly demonstrates that the statistical characteristics of the numerically generated surface agree with those given by Eq. (22). Since the aim of this paper is to understand the microscale texture transfer process in cold rolling, a digital form of rough surface was used in this study.

4 Results and discussion

4.1 Model verification

To verify the prediction given by the slab method and demonstrate its computational efficiency, the finite element method was also used to analyse cold rolling process. The uniaxial yielding Y_a of the strip used in the finite element analysis can be related to its yielding strength under plane strain condition by [3]

$$Y = \frac{Y_a}{\sqrt{3}} \tag{23}$$

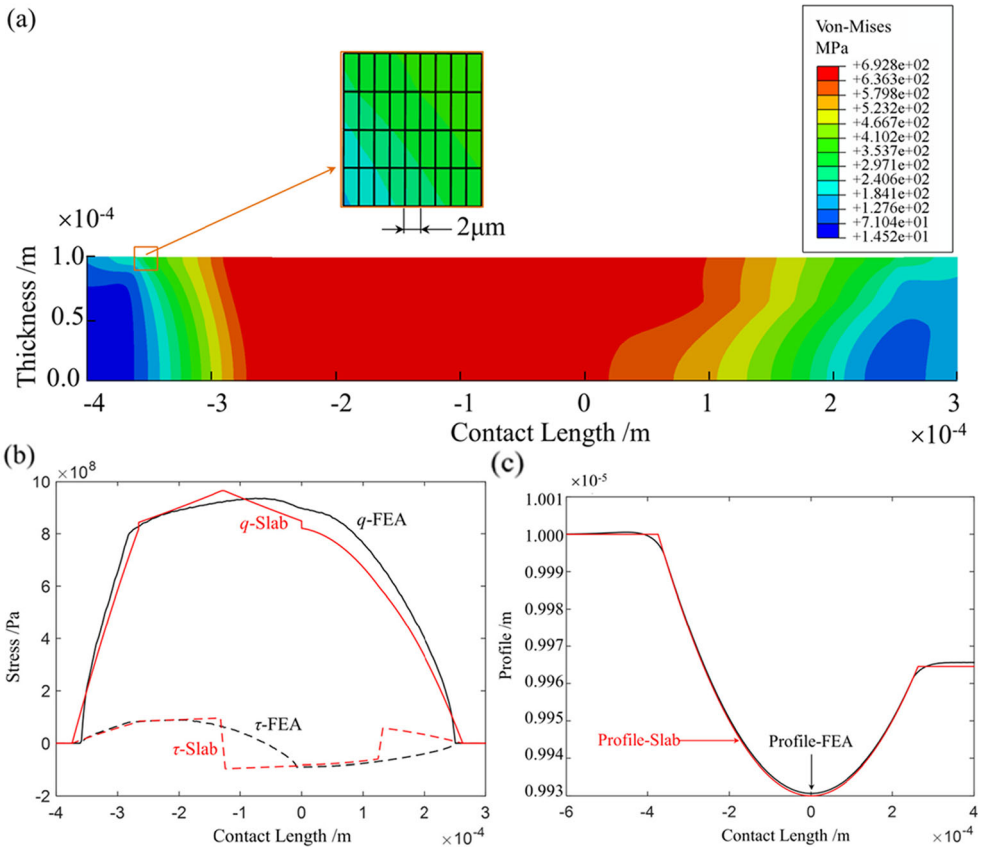

Fig. 6 Slab method vs finite element. **a** von-Mises predicted by FEA. **b** Interface stress comparison. **c** Predicted strip profile

To facilitate the comparison, a constant friction coefficient was used in both the FE and slab methods. The FEA was conducted by using a commercial FE package, ABAQUS EXPLICIT. Under the same rolling conditions (smooth roll surface, and zero front and back tensions), the calculated von-Mises stress distribution in the strip is given in Fig. 6a. Figure 6b compares the results from the slab and finite element methods. It demonstrates that the normal contact pressure given by the slab method agrees well with that predicted by the finite element method. The rolling forces given by the two methods are 448 N/mm and 426 N/mm, respectively, with a relative error of 4.94% only. Since a constant friction coefficient was used in the slab method, a sudden change in the direction of friction stress is not a surprise. Fig. 6c demonstrates the predicted strip profile under rolling given by the two methods, showing an excellent agreement. Some difference can be noted at the entry and exit because the slab method in this study did not consider the Saint-Venant's Principle. Although the influence of elastic strips outside the boundary of contact does not cease, it seems that such influence does not substantially affect the predicted rolled strip.

The calculations were conducted on a desktop PC with a processor of Intel (R) Core i5-3470 CPU @3.2 GHz. Using the proposed slab method (with MATLAB R2014b), the calculation took 5.3 s; but when using the finite element method (ABAQUS EXPLICIT 6.12-3), it consumed 762 s. Clearly, the proposed slab method is much more efficient.

4.2 Strip velocity

The strip velocity was calculated by using Eqs. (14) to (16). To verify this method, the predicted average strip velocity was compared with those given by the conventional

Table 1 Parameters used in the simulation

Name	Symbols	Value
Roll radius	R	0.1 m
Half strip thickness	y_1	1.0×10^{-4} m
Rolling Speed	V_{roll}	20 m/s
Yielding strength (Plane strain)	Y	400 MPa
Uniaxial yielding strength	Y_a	692.8 MPa
Young's' Modulus	E	210GPa
Poisson Ratio	υ	0.3
Creep velocity	V_{crit}	0.05 m/s
Coulomb friction coefficient	c_a	0.1
Entry velocity	u_1	19.88 m/s
Exit stress	σ_2	0 MPa
Roll roughness	$R_{q,roll}$	0.4 μm

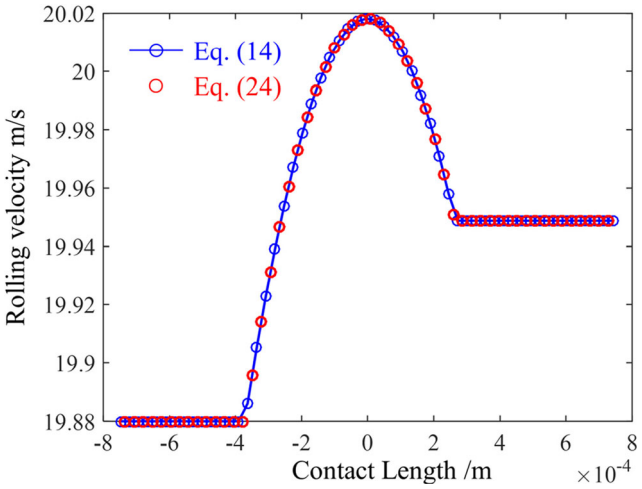

Fig. 7 Velocity verification ($\alpha = 0.7\%$)

method. By considering the conservation of material flow in the rolling bite, the average strip velocity can also be given by [12, 15, 16]

$$V_{ave} = \frac{y_1 u_1}{y} \tag{24}$$

The parameters for the numerical calculation of steady state rolling are listed in Table 1. Here, the roll surface roughness is set to be zero. Figure 7 shows that the strip velocity given by Eq. (14) agrees well with those given by the conventional approach.

4.3 Transient solution with surface roughness

With the method verified, the roll-to-strip texture transfer and its effect on the transient distribution of interface contact stresses could be accurately determined. The microscale surface roughness was generated randomly by MATLAB, as shown in Fig. 5c. In this study, the same surface roughness was used for all the calculations. The parameters for the transient simulation are listed in Table 1.

Figures 8, 9, and 10 show the transient distribution of the interface stresses as the roll surface roughness is drawn into the rolling bite. Figure 8 demonstrates the steady rolling without considering the texture transfer. It can be noted that the strip thickness in the rolling bite does not vary with respect to time, as shown in Fig. 8b. The predicted interface stresses are given in Fig. 8a. Because of the hybrid boundary conditions used, stress $\sigma_{x,\text{exit}}$ at the exit is zero while a negative stress at the entry is predicted due to the fixed entry slab velocity. As the roll surface roughness passes through the rolling bite, a non-continual distribution of interface stresses was observed, as shown in Fig. 9a. By carefully examining the strip profile, see Fig. 9b, it can be seen that there is no perfect contact between roll and strip surfaces. The amplitude of the roll surface roughness brings about non-continual contacts, which eventually leads to the non-continual distribution of stresses. Figure 10a, b show the transient interface stress and strip profile in the rolling bite after the rough roll surface has gone through the whole rolling bite. It is interesting to note that the surface roughness can considerably enlarge the contact length in comparison with a steady state rolling process. This is due to the fact that the random distribution of surface asperity heights on the roll surface led to the random contacts at the roll-strip interface. Thus, the contact outside the nominal contact zone can be expected, as evidenced in Fig. 9b.

Figure 11a illustrates the surface finish of a rolled strip, which demonstrates the results of the texture transfer from the work roll surface to the strip surface. Moreover, the deterministic surface finish of a rolled strip can be predicted as well by using the established method. Since the random distribution of surface roughness is considered, it is reasonable to see that the rolling force is also time-dependent. Figure 11b shows the evolution of the rolling force with respect to time when the instant texture transfer is taken into account. The rolling force can be calculated by integrating σ_y over the contact regime. The rolling force showed in Fig. 11b corresponds to the total

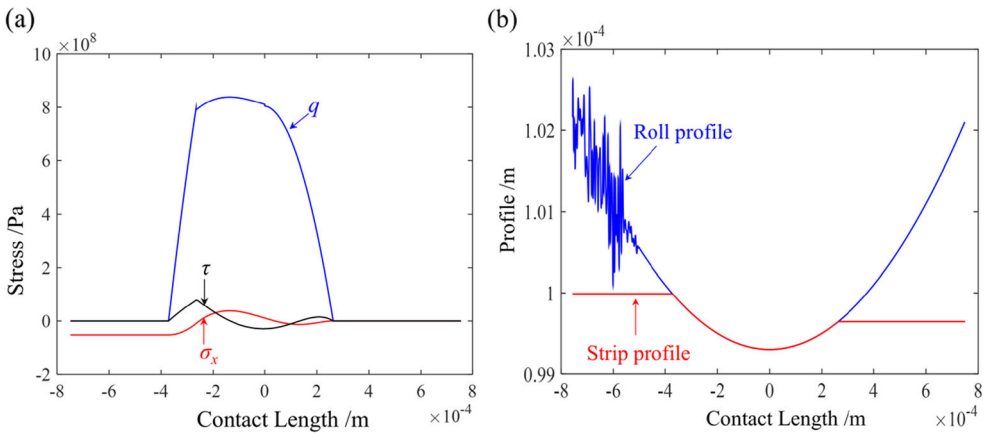

Fig. 8 Steady state ($\alpha = 0.7\%$). **a** Interface stress. **b** Strip profile

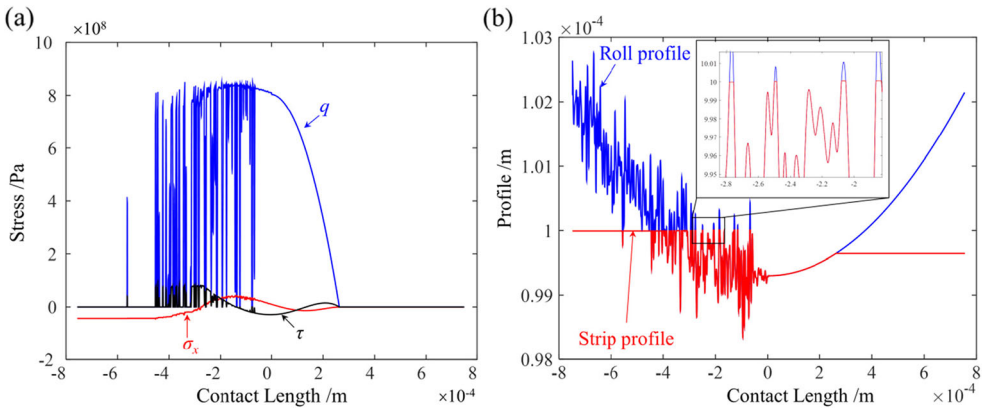

Fig. 9 Transient state under rolling ($\alpha = 0.7\%$). **a** Interface stress. **b** Strip profile

force per millimeter width of strip. It can be seen that the rolling force increases considerably to a peak before dropping to a level that is lower than the steady state as the surface roughness is drawn into the rolling bite. The time-dependent rolling force has demonstrated that the roll-to-strip texture transfer has a big influence on the rolling force.

4.4 Roughness transfer ratio

As discussed above, the roll-to-strip surface texture has been successfully predicted by using the method established above. Let us now see if the texture in the roll surface can be exactly transferred to the strip surface or not. This can be examined by introducing the roughness transfer ratio defined as follows:

$$\psi = \frac{R_q}{R_{q,roll}} \tag{25}$$

where R_q is the roughness on the rolled strip surface. To obtain ψ, a set of simulations were carried out. The reduction ratio of the strip is defined as

$$\alpha = \left|\frac{y_1 - y_0}{y_1}\right| \tag{26}$$

Figure 12 demonstrates the surface finish of the rolled strip with different reduction ratio α. For a small α, e.g., less than 0.1%, there is not noticeable texture transfer from the roll surface to the strip surface. This is due to the fact that the deformation of the strip in the rolling bite is mainly elastic. As the reduction ratio increases, the strip deforms plastically and the rolled strip surface becomes rougher because of the texture transfer process. It can be seen that the deterministic distribution of the surface finish varies substantially due to the increase in reduction ratio.

Figure 13a shows the effects of reduction ratio on the surface texture transfer. It can be see that the texture transfer ratio increases with increasing the reduction ratio. For the reduction ratio less than 0.7%, the texture transfer ratio varies nearly linearly with the reduction ratio. However, the texture transfer ratio will approach a plateau with a further increase in the reduction ratio. The elastic recovery of the strip material plays an important role in determining the surface finish, and makes the complete texture transfer impossible. Figure 13b shows the transient rolling forces with different reduction ratios. The rolling force increases substantially as the reduction ratio rises. However, the force always reaches its peak before decreasing for reduction ratios larger than 0.1%. With a small

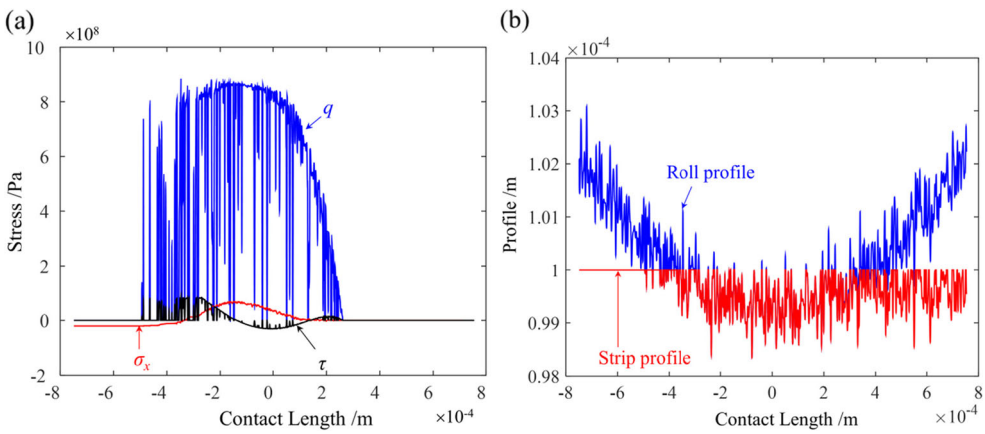

Fig. 10 Transient state with completed rolling ($\alpha = 0.7\%$). **a** Interface stress. **b** Strip profile

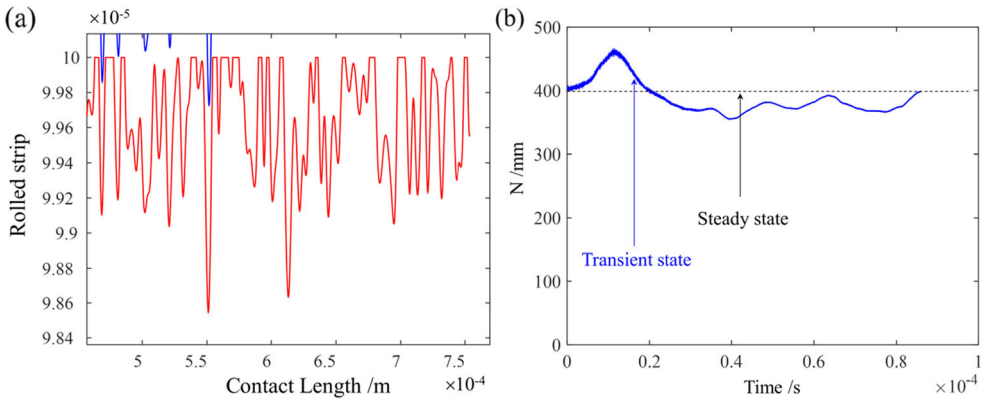

Fig. 11 **a** Surface finish on a rolled strip. **b** Transient rolling force per millimeter width

reduction ratio, e.g., − 0.1%, the rolling force increases monotonically as the roughness is drawn into the rolling bite and levels out after the roughness completely passes through the rolling bite.

By examining the results given by Figs. 12 and 13a, it is interesting to see that there is still some texture transfer at a negative reduction. The transient state of rolling in Fig. 14a shows that this is due to the surface roughness which causes some discrete contacts in the rolling bite, as illustrated in Fig. 14b. As the roughness passes through the rolling bite, only parts of the roll surface texture with high roughness amplitudes are in contact with the strip surface and cause the strip to deform plastically locally. This is more clearly demonstrated in Figs. 14c, d.

5 Conclusions

This paper has developed a simple approach to investigate the surface texture transfer in cold rolling. A transient model has been developed for analysing the non-steady state of rolling taking into account the instant texture transfer. A slab method with hybrid boundary conditions has been used to predict the interface stresses and strip profile. A numerically generated rough surface was used in the calculation. In order to account for the effects of instant texture transfer on rolling, a time forward method has employed and a multiple loading/unloading processes in each slab has been incorporated into the analysis. In addition, a finite element analysis was conducted to verify the interface stresses and strip profile under the same rolling conditions. With

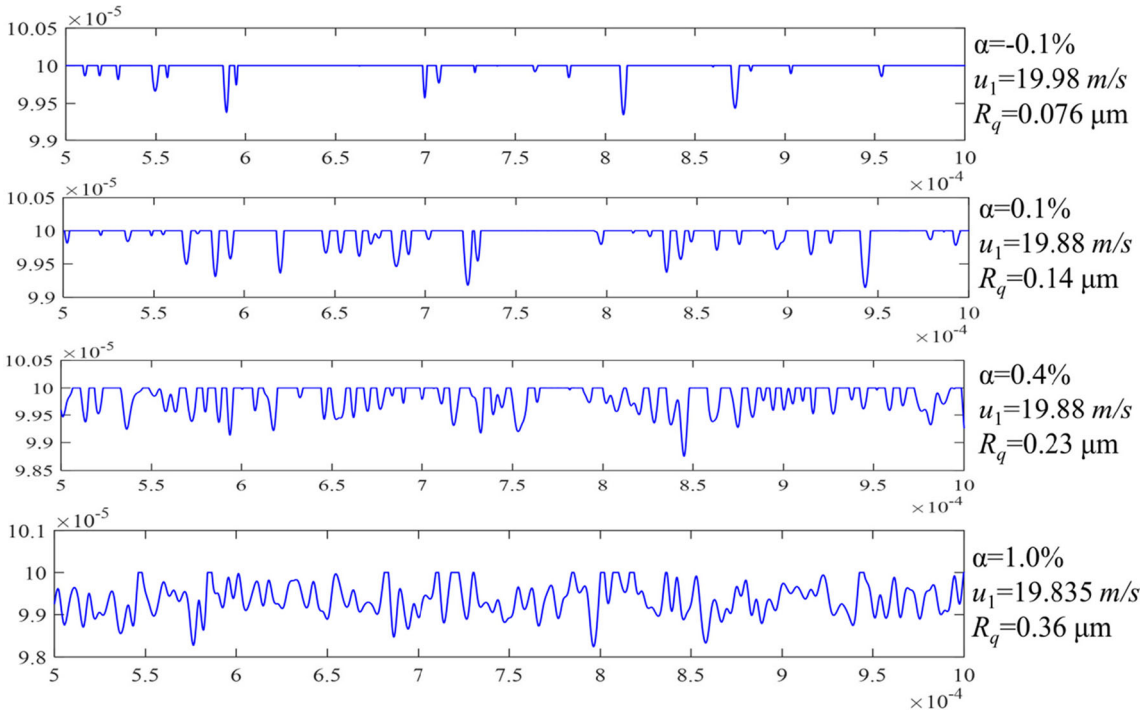

Fig. 12 Surface finish with different reduction ratio

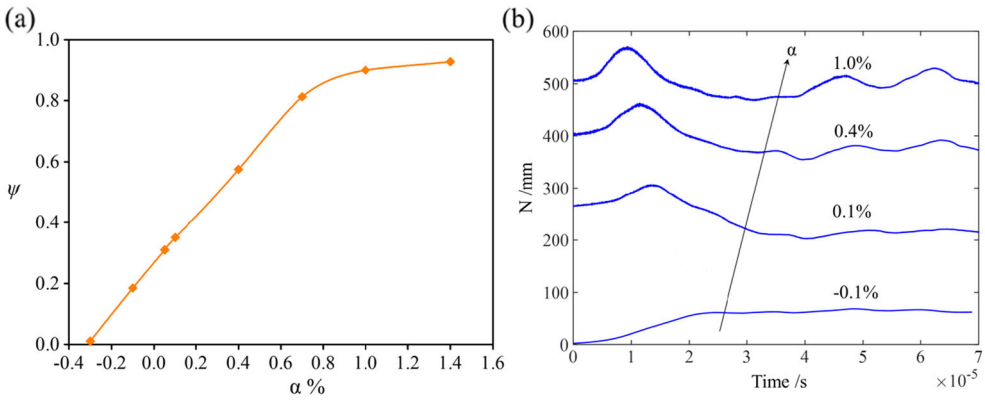

Fig. 13 **a** Transfer ratio plotted against the reduction ratio. **b** Reduction ratio effects on rolling force

the aid of this method, the roll-to-strip texture transfer and its effect on the transient distribution of interface stresses have been predicted. This approach has enabled us to deeply understand the effects of texture transfer on the cold rolling performance.

With the aid of the method established, the study has obtained the following major findings:

(i) Under the same rolling conditions, the interface contact stresses and strip profile predicted by the proposed slab method agree well with those given by the FEM. However, the former is much more efficient and cost-effective.

(ii) The random distribution of the surface asperity heights on a rigid work roll leads to discrete contacts at the roll-strip interface, which brings about a non-continual distribution of interface stresses. Moreover, the surface roughness enlarges the length of the rolling bite.

(iii) The surface texture of a work roll can be transferred to a strip surface in rolling. The texture transfer ratio

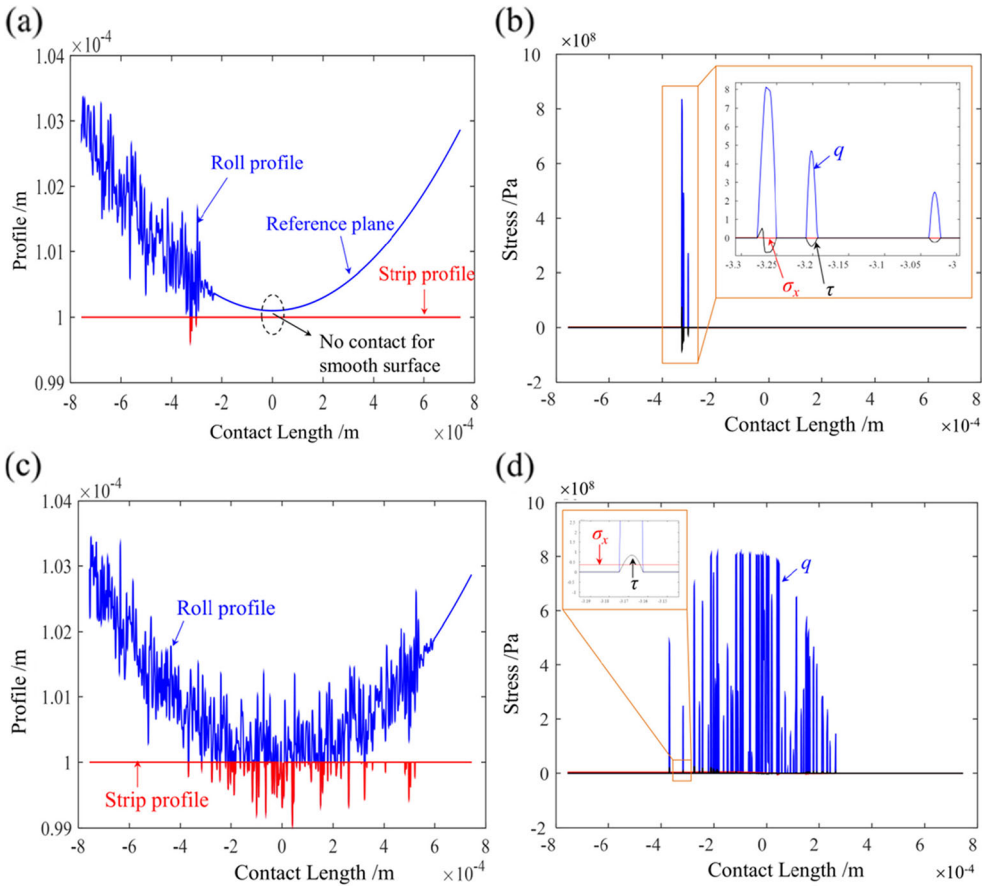

Fig. 14 Texture transfer with a negative reduction ratio ($\alpha = -0.1\%$). **a** Strip profile at the initial state. **b** Stresses at the initial state. **c** Strip profile at the completed state. **d** Stresses at the completed state

increases as the reduction ratio rises. The texture transfer ratio approaches a plateau because of the elastic recovery of the strip material.

(iv) Because of the instant roll-to-strip texture transfer, the rolling force is time-dependent. Moreover, the rolling force increases substantially as the reduction ratio increases. For a medium reduction ratio, the rolling force can reach a peak before decreasing when instant texture transfer is considered.

Funding information This research forms part of the Baosteel Australia Research and Development Centre (BAJC) portfolio of projects and has received support through the Centre, Project BA15001.

References

1. Von Karman T (1925) Contribution to the theory of rolling. Z Angew Math Mech 5:139–141
2. Bland DR, Ford H (1948) The calculation of roll force and torque in cold rolling with tension. Proc Ins Mech Eng 159:144–163
3. Alexander JM (1972) On the theory of rolling. In proceedings of the Royal Society of London a: mathematical. Phys Eng Sci 326:535–563
4. Fleck NA, Johnson KL (1987) Towards a new theory of cold rolling thin foil. Int J Mech Sci 29(7):507–524
5. Fleck NA, Johnson KL, Mear M, Zhang LC (1992) Cold rolling of foil. Proc Inst Mech Eng 201:119–131
6. Hwu Y, Lenard JG (1988) A finite element study of flat rolling. J Eng Mater Technol 110(1):22–27
7. Cavaliere MA, Goldschmit Marcela B, Dvorkin EN (2001) Finite element simulation of the steel plates hot rolling process. Int J Numer Methods Eng 52(12):1411–1430
8. Jiang ZY, Tieu AK, Zhang XM, Lu C, Sun WH (2003) Finite element simulation of cold rolling of thin strip. J Mater Process Technol 140(1):542–547
9. Hol J, Meinders VT, Geijselaers HJM, van den Boogaard AH (2015) Multi-scale friction 19odelling for sheet metal forming: The mixed lubrication regime. Tribol Int 85:10–25
10. Hol J, Meinders VT, Geijselaers HJM, van den Boogaard AH (2015) Multi-scale friction modelling for sheet metal forming: the boundary lubrication regime. Tribol Int 81:112–128
11. Wu CH, Zhang LC, Li SQ, Jiang ZL, Qu PL (2014) A novel multi-scale statistical characterisation of interface pressure and friction in metal strip rolling. Int J Mech Sci 89:391–402
12. Wu CH, Zhang LC, Li SQ, Jiang ZL, Qu PL (2016) A unified method for characterizing multiple lubrication regimes involving plastic deformation of surface asperities. Tribol Int 100:70–83
13. Wilson WRD, Sheu S (1988) Real area of contact and boundary friction in metal forming. Int J Mech Sci 30(7):475–489
14. Sutcliffe MPF (1988) Surface asperity deformation in metal forming processes. Int J Mech Sci 30(11):847–868
15. Wilson WRD, Chang DF (1996) Low speed mixed lubrication of bulk metal forming processes. J Tribol, ASME 118(1):83–89
16. Lin H, Marsault N, Wilson WRD (1998) A mixed lubrication model for cold strip rolling-part I: theoretical. Tribol Trans 41(3):317–326
17. Sutcliffe MPF, Johnson KL (1990) Lubrication in cold strip rolling in the mixed regime. Proc Inst Mech Eng B J Eng Manuf 204(4):249–261
18. Zhang S, Lenard JG (1992) The effects of the reduction, speed and lubricant viscosity on friction in cold rolling. J Mater Process Technol 30(2):197–209
19. Kijima H (2015) Influence of lubrication on roughness crushing in skin-pass rolling of steel strip. J Mater Process Technol 216:1–9
20. Ma B, Tieu AK, Lu C, Jiang Z (2002) An experimental investigation of steel surface characteristic transfer by cold rolling. J Mater Process Technol 125:657–663
21. Kijima H, Bay N (2008) Skin-pass rolling I-studies on roughness transfer and elongation under pure normal loading. Int J Mach Tools Manuf 48(12):1313–1317
22. Kijima H, Bay N (2008) Skin-pass rolling II-studies of roughness transfer under combined normal and tangential loading. Int J Mach Tools Manuf 48(12):1308–1312
23. Kijima H (2014) Influence of roll radius on roughness transfer in skin-pass rolling of steel strip. J Mater Process Technol 214(5):1111–1119
24. Johnson KL (1985) Contact Mechanics. Cambridege Univ. Press, UK
25. Le HR, Sutcliffe MPF (2001) A robust model for rolling of thin strip and foil. Int J Mech Sci 43(6):1405–1419